

Boundary effect on concrete fracture induced by non-constant fracture energy distribution

K.Duan & X.Z.Hu

Department of Mechanical & Materials Engineering, The University of Western Australia, 35 Stirling Highway, Crawley, WA 6009, Australia

F.H.Wittmann

Institute for Building Materials, Swiss Federal Institute of Technology, CH-8093 Zürich, Switzerland

ABSTRACT: This paper assumes that the fracture energy required to separate a unit crack area along the crack growth path is influenced by the width of the fracture process zone (FPZ) at that location. This assumption is based on considerations of the following fracture mechanisms: friction between the uneven upper and lower crack surfaces during crack opening and crack growth, micro-crack interactions within the FPZ. Instead of using a single constant fracture energy G_F for the entire projected fracture area, our present model assumes a bi-linear fracture energy distribution. G_F is constant if FPZ is fully developed and is not influenced by the specimen boundary, and G_F is linearly decreased if FPZ cannot be fully developed when approaching to the specimen boundary. That is the change in FPZ leads to the boundary or size effect on G_F . The present boundary effect model is compared with the other size effect models and experimental results.

1 INTRODUCTION

The size effects on fracture energy and strength of concrete have been studied extensively and various size effect models have been proposed (e.g. Bažant, 1984, Bažant, & Pfeiffer, 1987, Mindess, 1984, Nallathambi et al. 1984, 1985, Hillerborg, 1985, Wittmann et al. 1990, Carpinteri et al. 1994, Hu, 1997, 1998, Hu & Wittmann, 2000, Trunk, 2000). Much of these efforts is directed at the explanations why these fracture parameters vary with the specimen size or from small specimens to large concrete structures. Only few, such as a local fracture energy model (Hu, 1990, Hu & Wittmann, 1992), have addressed the possibility that the fracture energy itself may not be constant along the crack path in a concrete specimen.

In this paper, we assume a bi-linear fracture energy distribution to consider the boundary effect on the propagation of a fictitious crack in concrete. The fictitious crack with a large FPZ when approaching to the specimen boundary is forced to adopt itself to the stress field strongly influenced by the boundary. As a result, the FPZ size, measured by its length and width, is changed, leading to a variation in the fracture energy consumed in the fracture process of the boundary region. Therefore, in this paper we use the concepts of "boundary effects" and "local fracture energy distribution" to model the common size effects on the fracture properties of concrete.

2 LOCAL FRACTURE ENERGY

The specific fracture energy of concrete G_F is in fact an average energy measurement. According to the RILEM recommendation (RILEM, 1985), the specific fracture G_F is calculated by dividing the total applied energy with the projected ligament area. Therefore, for a specimen with a width W and an initial crack length a , the fracture energy G_F is given by:

$$G_F = \frac{1}{(W-a)B} \int P d\delta \quad (1)$$

where B is the specimen thickness, P is the applied load, and δ is the displacement at the loading point.

If a fictitious (or bridged) crack (Hillerborg, 1983) is used to model concrete fracture, the bridging (or cohesive) stress and crack opening (σ_b-w) relationship is related to G_F in the following way:

$$G_F = \int_0^{w_c} \sigma_b dw \quad (2)$$

where w_c is the critical crack opening above which, there is no more cohesive stress transferred. Obviously, G_F has to be a material constant. And it is wished equation (1) points out a simple way of measuring G_F in experiment.

Although it is widely known the specific fracture energy defined by equation (1), in spite of very sim-

ple, can be size dependent, few have ever questioned whether G_F defined by equation (2) is size dependent. To answer this question, we will firstly have to see how concrete softening occurs and what contributes to the (σ_b-w) relationship of concrete.

As illustrated schematically in Figure 1, the fracture process zone (FPZ) or damage zone around a propagating crack can be considered as consisting of two regions, an inner straining softening zone (W_{sf}), and an outer micro-fracture zone (W_f) (Hu, 1990, Hu & Wittmann, 1992). The inner softening zone W_{sf} contains inter-connected cracks along the aggregate and mortar interface, and interconnected cracks and defects in mortar and aggregates. The main crack plus a few large crack branches can be formed within the softening zone. The forming and complete separation of the softening zone control the (σ_b-w) relationship. The outer micro-fracture zone contains micro-cracks that are not interconnected, which do not contribute to the concrete softening. The fracture energy consumed in the outer micro-fracture zone is small, and equations (1) and (2) in principle should determine the same specific fracture energy.

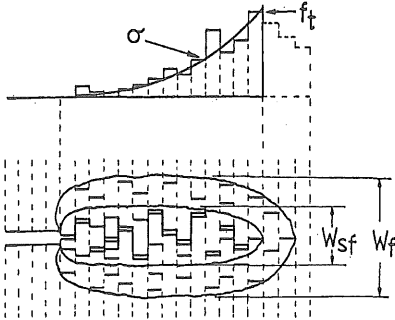


Figure 1. The FPZ and discrete bridging stresses. The FPZ is divided into the inner softening zone and the outer micro-fracture zone. w_c is related to the width of the softening zone W_{sf} (Hu & Wittmann, 1992)

However, during concrete fracture the inner and outer zones widths, W_{sf} and W_f , may vary according to the crack-tip stress field. As a result, variation in the critical crack opening w_c becomes inevitable. It becomes even more obvious when a FPZ is approaching to the boundary of a specimen, where the physical size of the remaining ligament and the high gradient stress field limit both the inner and outer zones, and thus their widths, W_{sf} and W_f . Therefore, a smaller w_c and a smaller fracture energy G_F as defined by equation (2) are found. This rationale leads to a logical conclusion that the specific fracture energy G_F defined by equation (2) can be location dependent because of the variations in W_{sf} , W_f and w_c . To distinguish the fracture energy G_F defined by

equation (2) from that defined by equation (1), we use the symbol g_f as the local fracture energy.

Let x indicate a position along the crack path, the local fracture energy $g_f(x)$ can be related to the local critical crack opening $w_c(x)$ and FPZ width by the following assumptions (Hu, 1990, Hu & Wittmann, 1992):

$$\begin{aligned} W_{sf}(x) &\propto W_f(x) \\ w_c(x) &\propto W_{sf}(x) \\ g_f(x) &\propto w_c(x) \end{aligned} \quad (3)$$

Furthermore, because the fracture energy defined by equation (1) may be size or ligament dependent, we use the symbol $G_f(a)$ to account for the size effects. The symbol G_F is only used if the specific fracture energy is size independent.

As shown in Figure 1, the fracture of a concrete specimen is equivalent to tensile failures of those assumed thin strips (small tensile specimens) in front of the crack tip. The specific fracture energy $g_f(x)$ for the small specimen at location x is determined by equation (2) using $w_c(x)$.

According to the energy conservation principle, the specific fracture energy $G_f(a)$ defined by equation (1) can be determined as follows:

$$G_f(a) = \frac{1}{(W-a)} \int_0^{W-a} g_f(x) dx \quad (4)$$

Differentiating equation (4) gives the local fracture energy $g_f(a)$ at the crack tip, i.e.

$$g_f(a) = G_f(a) - (W-a) \frac{dG_f(a)}{da} \quad (5)$$

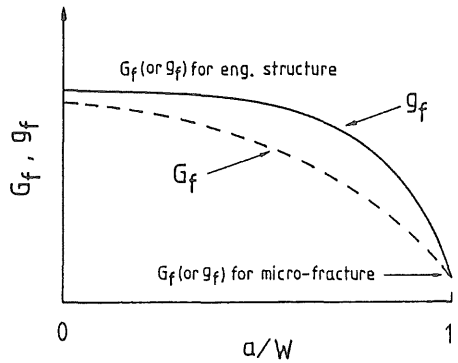


Figure 2. If g_f decreases monotonically along the ligament, G_f has to be dependent on the a/W ratio as observed in many experiments (Hu & Wittmann, 1992).

$g_f(a)$ and $G_f(a)$ in equation (5) have completely different meanings. $G_f(a)$ as defined by equation (1) is the averaged fracture energy determined by a specimen with an initial crack “ a ” while $g_f(a)$ is the local fracture energy at the crack tip (“ a ” becomes a location parameter).

It is clear from equations (4) and (5) that $G_f(a) = \text{constant} = G_F$, if $g_f(x) = \text{constant}$. If $g_f(x) \neq \text{constant}$, $G_f(a) \neq \text{constant}$, i.e. size or ligament effects are observed. Figure 2 shows schematically that if $g_f(x)$ decreases when approaching the boundary at the later stage of fracture, $G_f(a)$ is indeed ligament or initial crack length dependent. As normally $G_f(a)$ defined by equation (1) is measured for various a/W ratios, the local fracture energy distribution $g_f(x)$ can be determined by equation (5).

3 SPECIMEN SIZE EFFECT ON FRACTURE ENERGY

It has been confirmed by many researchers (Bažant & Lin, 1988, Hu, 1990, Hu & Wittmann, 1992, Otsuka et al. 1998) that the FPZ width was substantially decreased when the crack is approaching to the back surface of a specimen. The maximum FPZ width is established when the crack is far away from the boundary. And if a specimen is large enough, there exists a region the FPZ width is relatively constant.

To simplify the previous local fracture energy analysis (Hu, 1990, Hu & Wittmann, 1992), a bi-linear function can be assumed for $g_f(x)$, as shown in Figure 3. Figure 3a displays a specimen with the width W and an initial crack size “ a ”. A Cartesian system with its origin at the crack tip is attached to the specimen to assist the analysis. The bi-linear function consists of a horizontal line with the value of G_F and a descending line that reduces to zero at the back surface of the specimen. The intersection of these two straight lines is defined as the transition ligament a_l^* , a parameter depending on both the material properties and specimen geometry. For a specimen with a ligament size $(W-a)$ larger than the transition ligament a_l^* , $g_f(x)$ is given by:

$$g_f(x) = \begin{cases} G_F & x < W - a - a_l^* \\ G_F \left[1 - \frac{x - (W - a - a_l^*)}{a_l^*} \right] & x \geq W - a - a_l^* \end{cases} \quad (6)$$

If $(W-a)$ is smaller than the ligament transition length a_l^* , the first function in equation (6) disappears. Substitute equation (6) into (4), the size-dependent specific fracture energy is obtained,

$$G_f(a) = \begin{cases} G_F \left[1 - \frac{a_l^*}{2(W-a)} \right] & W - a > a_l^* \\ \frac{1}{2} G_F \frac{(W-a)}{a_l^*} & W - a \leq a_l^* \end{cases} \quad (7)$$

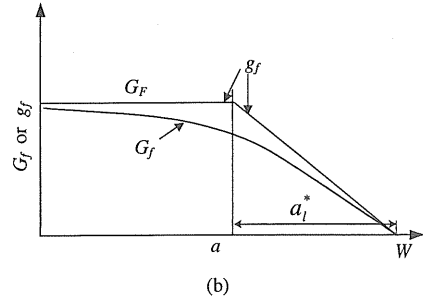
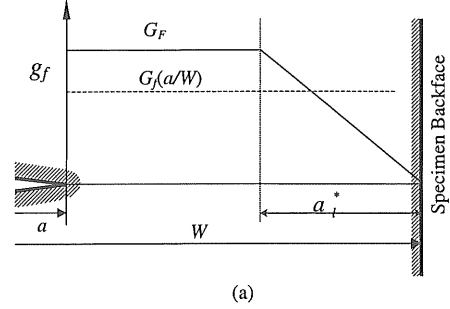


Figure 3. The distribution of fracture energy (G_f and g_f) along the ligament of a fracture mechanics specimen

It is clear from equation (7) that $(W-a)$ has to be much larger than the transition ligament a_l^* to avoid the ligament or size effect. Since the size parameter “ W ” is often used when the specimen size effect on the fracture energy is considered, equation (7) can be rewritten as:

$$G_f \left(\frac{a}{W} \right) = \begin{cases} G_F \left(1 - \frac{1}{2} \cdot \frac{a_l^*/W}{1-a/W} \right) & 1 - a/W > a_l^*/W \\ G_F \cdot \frac{1}{2} \cdot \frac{(1-a/W)}{a_l^*/W} & 1 - a/W \leq a_l^*/W \end{cases} \quad (8)$$

Equations (7) and (8) can be better understood from the sketch shown in Figure 3. If a specimen with a width “ W ” and an initial crack “ a ” is used to measure the fracture energy according to the RILEM standards (1985), an average value $G_f(a/W)$ is obtained. $G_f(a/W)$ is a/W ratio dependent. Although the a/W ratio is always used when the size effects on concrete fracture is considered, Figure 3 suggests it may not be always appropriate. For the convenience

of discussion, we assume for the time being that the transition ligament a_l^* is constant. If $W \gg a_l^*$, and $(W-a) \gg a_l^*$, $G_f(a/W) = \text{constant} = G_F$. But for the same large specimen ($W \gg a_l^*$), the size effect is still possible if $(W-a) \approx a_l^*$. That is the boundary effect exists, and it is not enough to consider only the absolute physical size W of a specimen.

As shown in Figure 3, if we change the initial crack length from “ a ” to “ W ”, a $G_f(a)$ or $G_f(a/W)$ curve is obtained, showing the ligament effects on the fracture energy – a phenomenon has been frequently observed in experiment.

From Figure 3, we know the upper limit of $G_f(a/W)$ is the size independent fracture energy G_F . Figure 3 also tells us that testing of very large concrete specimens is not necessary, because G_F can be worked out from the size dependent $G_f(a/W)$ as long as $(W-a) > a_l^*$. That is the key assumption and major contribution of the current bi-linear local fracture energy model.

4 ANALYSIS OF EXPERIMENTAL OBSERVATIONS

4.1 Fracture energy of a mortar by wedge splitting test

We chose the following example to illustrate the application of equations (6) to (8).

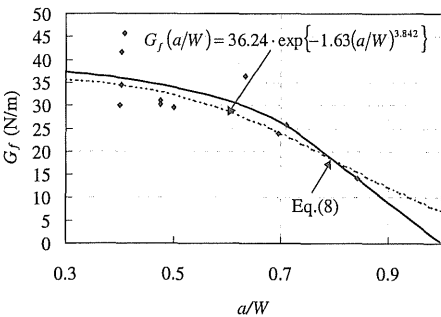


Figure 4. The comparison of the predictions from equation (8) and the best fit with the measured fracture energy data given in ref. (Hu, 1990).

Figure 4 shows the fracture energy measurements of a fixed size W , but with various a/W ratios method (Hu, 1990, Hu & Wittmann, 1992). Clearly, the fracture energy of the mortar with the maximum sand size of 1 mm tested under the wedge splitting condition is not constant.

Hu and Wittmann used the following two functions to curve-fit their data,

$$G_f(a/W) = 36.2 \cdot \exp\{-1.63(a/W)^{3.84}\} \quad (9)$$

and

$$G_f(a/W) = 43.88 - \frac{5.20}{1 - a/W} \quad a/W < 0.7 \quad (10)$$

Equation (9) is also shown in Figure 4.

By applying equation (7) or (8) to these measured G_f data, the size-independent fracture energy G_F and the transition ligament a_l^* are determined to be 45.71 N/m and 46 mm, respectively. The predicted G_F is in a good agreement with 43.88 N/m given in the earlier studies (Hu, 1990, Hu & Wittmann, 1992).

The predictions using the estimated parameters, G_F of 45.71 N/m and a_l^* of 46 mm, are plotted in Figure 4 to compare with those measured and best fitted G_f values. It is found that the prediction using equation (8) is superior to the best fit given by equation (9). Particularly, at high a/W ratios, this equation gives a correct physical trend that has been well documented, i.e. fracture energy required to break a ligament is reduced to zero when the notch tip approaches the back surface of the specimen (e.g. Cotterell & Mai, 1996).

By substituting equations (9) and (10) into equation (5), two g_f functions can be obtained as

$$g_f(a/W) = 36.2 \cdot \exp\{-1.63(a/W)^{3.84}\} \times \{1 + 6.26(a/W)^{2.84}(1 - a/W)\} \quad (11)$$

and

$$g_f(a/W) = \begin{cases} 43.9 & a/W \leq 0.7 \\ 124.8 - 115.6(a/W) & a/W > 0.7 \end{cases} \quad (12)$$

$g_f(a/W)$ function from the present study is calculated by setting $x = 0$, $G_F = 45.71$ N/m and $a_l^* = 46$ mm in equation (6),

$$g_f(a/W) = \begin{cases} 45.71 & a/W \leq 0.744 \\ 178.71(1 - a/W) & a/W > 0.744 \end{cases} \quad (13)$$

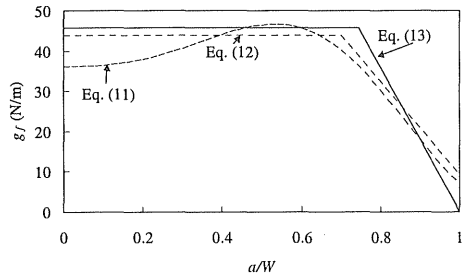


Figure 5. The g_f curves predicted by using these two best fit equations, and the present model.

The g_f predictions from these three equations are plotted in Figure 5. It can be seen here that the maximum g_f value of equation (11) is significantly smaller than the size-independent G_F , which is different from the definition of the parameter (Hu & Wittmann, 1992). Both equations (11) and (12) do not tend to zero when approaching the back free surface. On a contrast, the prediction from equation (13) satisfies both conditions.

4.2 Fracture properties of concrete by 3-point bending test

Nallathambi et al (1984, 1985) completed a series of fracture mechanics tests on concrete with different mixes using 3-point bending method. Their observations showed that while many factors such as aggregate texture and water/cement ratio contribute to fracture energy, specimen geometry played a dominant role in determining the fracture energy or fracture toughness value. Their experiments clearly showed that the ratio of specimen depth W to span had a significant effect on the fracture energy while other conditions are identical. Therefore, here a set of fracture energy data of 20 mm mix with identical depth-to-span ratio of 1/6 are chosen to compare with equation (8) as shown in Figure 6. The size-independent fracture energy G_F and transition ligament length a_l^* calculated from the results of these four groups of specimens with depths of 150, 200, 250 and 300 mm are listed in Table 1.

Table 1: Estimated specific fracture energy G_F and ligament transition length a_l^* from [19] for the beams with different depths.

W (mm)	G_F (N/m)	a_l^* (mm)
150	129.5	80.6
200	139.6	106.7
250	134.1	117.9
300	129.0	131.4

The predictions based on the parameters in Table 1 are plotted in Figure 6, and show a good agree-

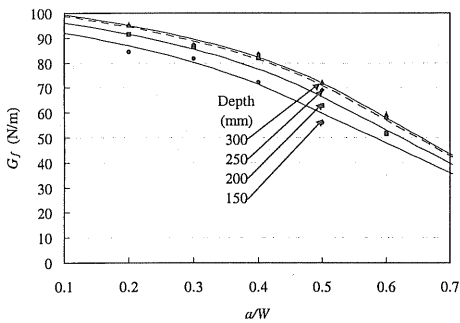


Figure 6. The comparison of the predictions from equation (8) with the measured fracture energy data given in refs. (Nallathambi et al. 1984, 1985).

ment with the experimental data. The largest difference between the predicted curves occurs at around $a/W = 0.5$, and these curves come closer when a/W moves away from this value. This is consistent with the physics behind these curves as all these curves will tend to zero when approaching the back boundary, and to the G_F when crack size is rather small.

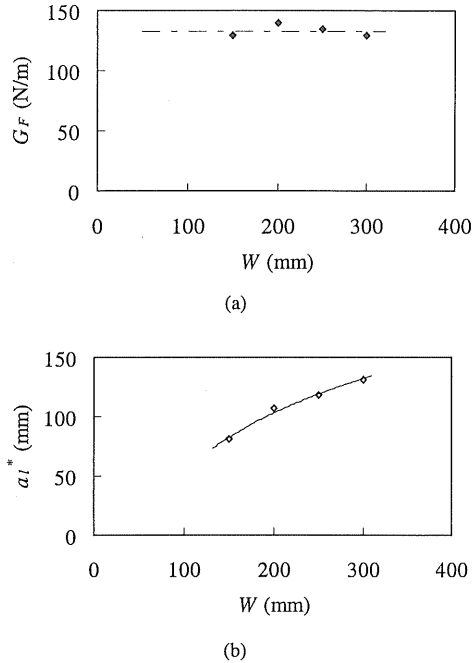


Figure 7. The size-independent fracture energy G_F and the transition ligament a_l^* as function of specimen depth W , predicted using equation (8).

To clarify the influence of specimen size on the fracture mechanics parameters in equations (7) and (8), the predicted G_F and a_l^* values are plotted against beam depth in Figure 7. It can be clearly seen that the specific fracture energy G_F calculated by equation (8) remains constant or size independent though the transition ligament a_l^* varies quite a lot for the tested specimen size range. Therefore, the fracture energy G_F of the concrete is determined as 133 N/m by averaging the four values.

The size influence on the ligament transition length a_l^* is in fact the size influence on the FPZ as previously discussed. It is quite possible that the ligament transition length a_l^* will reach to a maximum value, above which it is a size-independent material constant if W is further increased.

Substituting G_F of 133 N/m and different a_l^* values into equation (6), the g_f curves for different beam depths can be obtained as plotted in Figure 8.

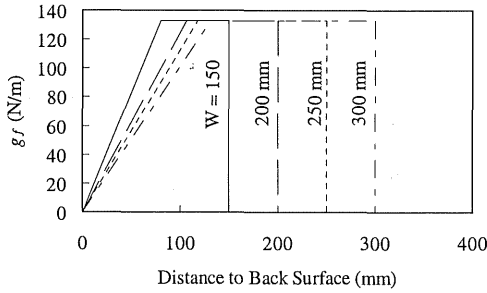


Figure 8. The g_f curves for the concrete beams with different depths.

It can be seen here that although the transition ligament a_l^* increases with the beam depth, the region of the maximum fracture energy G_F quickly becomes dominant contribution to the $G_f(a/w)$ measurements.

5 FURTHER DISCUSSIONS ON BOUNDARY EFFECTS

The bi-linear local fracture energy model presented in this paper is based on the previous local fracture energy (Hu 1990, Hu and Wittmann 1992). Both models are based on the consideration of proportionality of the local fracture energy to the FPZ width. However, the current bi-linear local fracture energy model has a clearer physical basis by introducing the transition ligament length a_l^* . This allows the direct evaluation of the size independent fracture energy G_F from the size dependent fracture energy results. More important, the introduction of the transition ligament length a_l^* has helped us to identify that the normal size or ligament effect is actually induced by the boundary effect.

The back boundary of a specimen eases the stresses in its vicinity, and therefore, reduces the FPZ width. As a result, the local fracture energy decreases rapidly when approaching the back surface. The extent of the region where the FPZ is perturbed by the back boundary is dependent on both the material properties and specimen geometry.

Because of the perturbation of back free surface on the g_f distribution along the ligament, the fracture energy G_f exhibits size effect behaviour. The G_f value is dependent on the position of the crack tip related to the back boundary. When the distance of the crack tip to the back free surface is comparable to the transition ligament a_l^* , the back boundary-perturbed g_f contributes significantly to the G_f . As a result, the G_f value is significantly less than the size-independent G_F . On other hand, when the crack tip is very far away from the back surface, the contribution of the perturbed g_f distribution is negligible, and the measured G_f will be very close to the size independent G_F .

In the previous studies, Hu and Wittmann (Hu, 1998, Hu & Wittmann, 2000) investigated the size effect on the fracture properties of a large plate with a finite crack and proposed an asymptotic solution to describe the dependence of specimen strength on the crack length,

$$\sigma_N = \frac{f_t}{\sqrt{1 + a/a_\infty^*}} \quad (14)$$

where σ_N is the nominal strength of the specimen and f_t , material tensile strength. a_∞^* is defined by the intersection of the maximum tensile stress and linear elastic fracture mechanics (LEFM) criteria, and is referred to as the reference crack size. The reference crack size a_∞^* represents an ideal brittle/ductile fracture transition.

For the large plate case, the crack size a represents the distance of the crack tip to the specimen front free surface. Equation (14) indicates that when the distance of the crack tip to the front boundary is comparable to the a_∞^* , the specimen strength will subject to the boundary effect. When the crack tip is very far away from the front boundary, the LEFM criterion prevails and the specimen strength is mainly determined by its fracture toughness K_{IC} . This analysis indicates that the size effect in the fracture of the large plate is also a (front) boundary effect phenomenon. Therefore, by proposing the current boundary effect mod and concept, it is possible to develop a general fracture mechanics model to cover various size/ligament effects on concrete fracture.

6 CONCLUSIONS

This paper explains the fundamental difference between equations (1) and (2). While equation (1) represent an averaged fracture energy, equation (2) really indicates a local fracture energy. The G_F values are equal only if the local fracture energy can remain constant for most of crack path.

As the previous local fracture energy model, the current paper also assumes that the local fracture energy will vary when the development of FPZ is affected. By introducing the concept of boundary effects and bi-linear local fracture energy distribution, the size or ligament effect on the fracture energy of concrete is explained. The important parameter is the transition ligament length a_l^* .

The bi-linear boundary effect model, equation (7) or (8), also shows that the absolute physical size measurement W is not sufficient in explanation of the size effect. This is because the boundary effect (and thus the size effect) still exists if $(W-a) \approx a_l^*$,

even if $W \gg a_l^*$. This clearly demonstrates the significance of $a_l^*/(W-a)$ in size effects of concrete fracture.

REFERENCES

- Bažant, Z. P. 1984. Size effect in blunt fracture: concrete, rock, metal. *Journal of Engineering Mechanics(ASCE)* 110(4): 518-535.
- Bažant, Z. P. & Lin, F.-B. 1988. Nonlocal smeared cracking model for concrete fracture. *Journal of Structural Engineering (ASCE)* 114: 2493-2510.
- Bažant, Z. P. & Pfeiffer, P. A. 1987. Determination of fracture energy from size effect and brittleness number. *ACI Materials Journal* 84 : 463-480.
- Carpinteri, A., Chiaia, B. & Ferro, G. 1994. Multifractal scaling law for the nominal strength variation of concrete structures. In M. Mihashi, H. Okamura & Z. P. Bažant (eds), *Size Effect in Concrete Structures*: 173-185. E&FN Spon.
- Cotterell, B. & Mai, Y.-W. 1996. *Fracture Mechanics of Cementitious Materials*. Blackie Academic & Professional.
- Higgins, D. D. & Bailey, J. E. 1976. Fracture measurements on cement paste. *Journal of Materials Science* 11: 1995-2003.
- Hillerborg, A. 1983. Analysis of one single crack. In F. H. Wittmann (ed), *Fracture Mechanics of Concrete*: 223-249. Amsterdam: Elsevier.
- Hillerborg, A. 1985. Results of three comparative test series for determining the fracture energy G_F of concrete. *Materials and Structures* 18: 33-39.
- Hu, X. Z. 1990. *Fracture Process Zone and Strain Softening in Cementitious Materials*. ETH Building Materials Reports No.1, ETH Switzerland. (AEDIFICATIO Publishers, 1995).
- Hu X. Z. 1997. Toughness measurements from crack close to free edge. *International Journal of Fracture*.86: L63-L68.
- Hu, X.Z. 1998. Size effects in toughness induced by crack close to free edge. In H. Mihashi and K. Rokugo (eds.), *Fracture Mechanics of Concrete Structures (Proc. FRAMCOS-3)*: 2011-2020. Freiburg: AEDIFICATIO Publishers.
- Hu, X. Z. & Wittmann, F. H. 1992. Fracture energy and fracture process zone. *Materials and Structures(RILEM)* 25: 319-326.
- Hu, X. Z. & Wittmann, F. H. 2000. Size effect on toughness induced by crack close to free surface. *Engineering Fracture Mechanics* 65: 209-211.
- Mindess, S. 1984. The effect of specimen size on the fracture energy of concrete. *Cement and Concrete Research* 14: 431-436.
- Nallathambi, P., Karihaloo, B. L. & Heaton, B. S. 1984. Effect of specimen and crack sizes, water/cement ratio and coarse aggregate texture upon fracture toughness of concrete. *Magazine of Concrete Research* 36(129): 227-236.
- Nallathambi, P., Karihaloo, B. L. & Heaton, B. S. 1985. Various size effects in fracture of concrete. *Cement and Concrete Research* 15: 117-126.
- Otsuka, K., Date, H. & Kurita, T. 1998. Fracture process zone in concrete tension specimens by x-ray and ae techniques. In H. Mihashi and K. Rokugo (eds.), *Fracture Mechanics of Concrete Structures (Proc. FRAMCOS-3)*: 3-16. Freiburg: AEDIFICATIO Publishers.
- RILEM TC-50 FMC. 1985. Determination of the fracture energy of mortar and concrete by means of three-point bend tests on notched beams. *Materials and Structures(RILEM)* 18: 287-290 (Endorsed May 1993).
- Trunk, B. 2000. *Einfluss der Bauteilgröße auf die Bruchenergie von Beton*. ETH Building Materials Reports No.11, ETH Switzerland. (AEDIFICATIO Publishers, 2000).
- Wittmann, F. H., Mihashi, H. & Nomura, N. 1990. Size effect on fracture energy of concrete. *Engineering Fracture Mechanics* 35: 107-115.